Energy consumption and product release characteristics evaluation of oil shale non-isothermal pyrolysis based on TG-DSC

Energy consumption and product release characteristics evaluation of oil shale non-isothermal pyrolysis based on TG-DSC

Shuai Zhao [a,b,c], Youhong Sun [a,b,c,*], Xiaoshu Lü [a,b,c,d,e], Qiang Li [a,b,c,*]

[a] *Construction Engineering, College of JiLin University, ChangChun, 130000, China*
[b] *National-Local Joint Engineering Laboratory of In-situ Conversion, Drilling and Exploitation Technology for Oil Shale, Changchun, Jilin, 130021, China*
[c] *Key Laboratory of Drilling and Exploitation Technology in Complex Condition, Ministry of Land and Resource, Changchun, Jilin, 130026, China*
[d] *Department of Electrical Engineering and Energy Technology, University of Vaasa, P.O.Box 700, FIN-65101, Finland*
[e] *Department of Civil Engineering, Aalto University, P.O.Box. 11000, FIN-02130, Finland*

Abstract

Thermogravimetric-Differential Scanning Calorimetry Analysis (TG-DSC) was applied to study non-isothermal pyrolysis characteristics of oil shales, such as the starting point, stability, pyrolysis interval and product release using Fuyu and Huadian oil shale samples. Results show that with the increase of heating rate, oil shale pyrolysis moves to higher temperature zone. This trend is more noticeable at higher oil content. The pyrolysis stability of the oil shale is related to oil content and pyrolysis atmosphere. The higher the oil content, the more stable the pyrolysis of the oil shale. Under nitrogen atmosphere, the pyrolysis interval of oil shale is more concentrated, air prolongs the pyrolysis interval, and the pyrolysis stability index decreases. In addition, the increase of heating rate favours the release characteristic index of the product, which is not practically affected by oil content. The release characteristic indices of pyrolysis products from oil shale under nitrogen atmosphere are higher than those under air atmosphere. The optimum heating rate that produces the highest oil product yield for pyrolysis progress of Huadian oil shale is 20 ^{o}C/min, and Fuyu oil shale is 40 ^{o}C/min.

Keywords: Oil shale; TG-DSC; Pyrolysis characteristics; Product release characteristic index; Heating rate and atmosphere

1. Introduction

Unlike traditional fossil energy sources such as coal, oil and natural gas, oil shale belongs to unconventional oil and gas resources. Oil shale is rich in kerogen, but it is a type of immature

material for hydrocarbon generation. High temperature pyrolysis can produce oil and gas products (Omar S et al., 2010). The types and maturity of kerogen in oil shale vary across different areas, so the hydrocarbon generation characteristics of kerogen are different under high temperature pyrolysis. In aerobic condition, oil and gas products can participate in the pyrolysis process further, resulting in serious product dissipation with low oil content and low recovery efficiency for oil and gas. Anaerobic pyrolysis is a process of kerogen pyrolysis, where no oxygen is involved and hence no organic matter is oxidized. Compared with aerobic pyrolysis, anaerobic pyrolysis can improve the recovery efficiency of kerogen pyrolysis products. Thermogravimetric-differential scanning calorimetry analysis (TG-DSC) provides general information about the overall reaction kinetics. This method has been widely used to investigate isothermal and non-isothermal pyrolysis characteristics of fossil fuels. While dealing with uncertainties of oil shale pyrolysis intervals has always remained one of biggest challenges in oil shale research, today fuzzy intervals have been used to handle uncertainties of pyrolysis intervals. Pyrolysis kinetics was also investigated by TG-DTG (Bai et al., 2017; Xiong et al., 2015; Wang et al., 2012). These techniques cannot fully explain the relationship between maturity, oil content and temperature distribution of oil shale pyrolysis. Zhang et al. (2018) showed that the range of variability in the principal activation energy is 200–242 kJ mol^{-1}, with most samples being in the middle half of that range, and the most-likely range of frequency factors is 1012-1016 s^{-1}, with most values being in the middle half of that range. Sun et al. (2015) studied pyrolysis kinetics of multi-stage parallel reaction for Huadian oil shale at different heating rates and particle sizes. The results showed that increases in particle size or heating rate shifted the combustion process to a higher temperature, because of mass transfer resistance and thermal hysteresis. Juliana et al. (2017) studied the devolatilization kinetics in pyrolysis of oil shale from the Irati Formation in Brazil. The results showed that kinetic parameters were determinable over the temperature range of 323–1173 K by dynamic thermogravimetric analysis using different model-free methods.

Evaluation and validation were performed for pyrolysis at 673 K for 3 h. It was found that the activation energy depended on the extent of conversion. Activation energy increased in the ranges 215–255 kJ mol^{-1} and $0.15 \leq \alpha \leq 0.55$ for conversion, where $\alpha=1$ for pyrolysis at 1173 K. Bao et al. (2019) conducted detailed study of the enhanced oil recovery techniques focusing on the recent ten years. As an important flow and oil recovery mechanism, molecular diffusion was studied and empirical correlation and experimental measurements were carried out. The influence of the structure of the porous media on the calculation results of the model was also considered. Oil shale is a low-quality oil and gas resource with low oil content. Only when the economic cost of investment is low, can it have exploitation value. Therefore, understanding and modeling the relationship between kerogen maturity, oil content and pyrolysis interval of oil shale under different atmospheric conditions and heating rates is a key element of any control process of oil shale, including in-situ pyrolysis temperature and the pyrolysis dissipation, for improving oil and gas recovery efficiency. In situ pyrolysis of oil shale triggered by topo chemical reaction is a complex chemical reaction process. At the initial stage, the pyrolysis of kerogen is caused by the introduction of high temperature nitrogen gas, and then the nitrogen gas is switched to air to promote further decomposition of kerogen. During this stage, oxidation reaction occurs and a large amount of heat is released, which continuously enhances the pyrolysis of oil shale in the formation process. This involves the precipitation properties of

products in different combustion intervals. Therefore, the pyrolysis properties of oil shale in Fuyu and Huadian areas of Jilin Province were studied by TG-DSC. The specific objectives are: 1. Introducing pyrolysis stability and product release characteristics to explain the reaction process and results in the pyrolysis interval of oil shale at different heating rates. 2. Studying effects of oil content, heating rate and pyrolysis atmosphere (nitrogen and air) on the starting point, pyrolysis stability, pyrolysis interval and product release characteristics of oil shale pyrolysis. 3. Calculating the exothermic behavior (exothermic and exothermic rate) of pyrolysis zone, which is influenced by oil content, heating rate and pyrolysis atmosphere, using DSC analysis. This can provide a reference for in-situ pyrolysis of local chemical oil shale.

2. Materials and methods

2.1. Materials

The Huadian oil shale samples used in the experiment are from the 9–13 layers of brown oil shale in Gongchengtou mining area, Huadian, Jilin Province. Gonghuangtou mining area is located in Huadian Basin. Its sedimentary thickness is 240–350 m. The upper part is pyrite deposit, and the lower part is carbonaceous mudstone deposit. It belongs to horizontal bedding development. Fuyu oil shale samples come from 466 to 487 m interval of FK-3 Well in Fuyu-Changchunling area of Songliao Basin. The oil shale in this section has been developed in the Upper Cretaceous Qingshankou Formation, which belongs to the semi-lake-deep lake environment and presents horizontal bedding. The samples were ground before the test. In order to avoid the influence of different particle sizes on the test results, the grinded oil shale samples were sieved into uniform particle sizes. The samples were dried at a constant temperature 60 ^{o}C oven to a constant weight, and then stored in a dryer for later use. The results of Proximate analysis, Element analysis and Fisher analysis are shown in Table 1.

Table 1 Analysis of oil shale in Fuyu and Huadian.

Attribute	Proximate analysis/wt.%			
Region	Moisture	Ash	Volatiles	Fixed carbon
FY	3.75	68.71	21.37	3.75
HD	1.12	54.26	43.24	1.38

Attribute	Fisher analysis/wt.%				Element analysis/wt.%			
Region	Shale oil	Water	Residue	Gas	H	C	N	S
FY	4.16	5.85	83.32	3.15	7.27	4.96	0.34	1.09
HD	18.31	3.79	67.39	10.51	4.02	28.86	0.64	2.12

Kerogen in oil shale is mainly filled with inorganic mineral skeleton. FTIR and XRD are often used to characterize organic and inorganic minerals in oil shale samples. Molecular structures of the samples are analyzed by investigating different groups of characteristic peaks (Bai et al., 2013; Sun et al., 2014).

Fig. 1 (a) shows the infrared spectra of Fuyu and Huadian oil shale. The mineral peaks are the most obvious in the spectra of the two kinds of oil shales, and their shapes are similar, which indicates that the mineral composition and content of the two kinds of oil shales are similar. The stretching vibration peak of Si–O bond is 1170–1060 cm^{-1}, which is formed by the overlapping absorption bands of quartz and clay minerals kaolinite, illite and montmorillonite in the oil shale. The characteristic absorption peaks are 804–780 cm^{-1} for quartz, 520-480 cm^{-1} for kaolinite, illite and montmorillonite, and 1430 and 877 $cm^{-1}$for calcites, respectively. Because the mineral content in oil shale was much higher than that of organic matter, the characteristic peaks of a large number of minerals could cover up part of the organic matter peaks. In the infrared spectra of Fuyu and Huadian oil shale, there are many vibration peaks of organic and mineral groups. The most obvious absorption peaks of these two kinds of oil shale organic matter were 2925 and 2850 cm^{-1}. That was the characteristic absorption peaks of aliphatic hydrocarbons, indicating that the main component of organic matter in oil shale is aliphatic hydrocarbons. The skeleton vibration of aromatic ring was 1620 cm^{-1} and the stretching vibration of C–O group was 1710 cm^{-1}. Vibration intensities of aliphatic transmission peaks and aromatic characteristic peaks were related to the content of kerogen in samples and the maturity of oil shale. This indicates that the kerogen of Fuyu and Huadian oil shales was mainly composed of aliphatic group, but not very mature. They were lacustrine deposits (Altun et al., 2009; Dong et al., 2018).

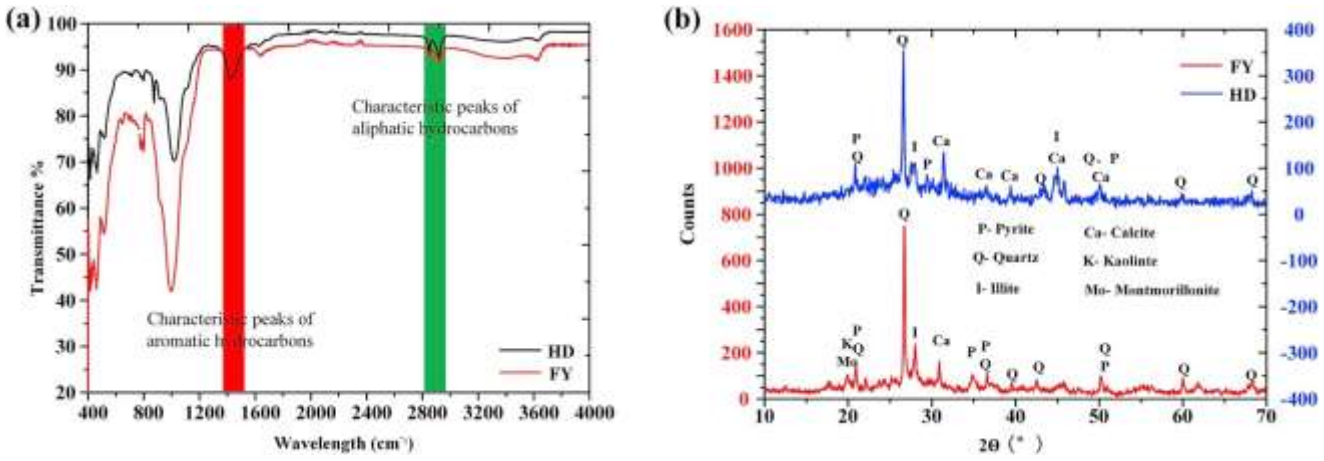

Fig. 1. FTIR and XRD maps of Fuyu and Huadian oil shales.

XRD and FTIR results of oil shale samples were mutually correlated, especially in the context of their inorganic minerals. As shown in Fig. 1 (b), the main mineral compositions of Fuyu and Huadian oil shale were: quartz, calcite, pyrite, feldspar and immense mixtures. Except that calcite was a carbonate mineral, other minerals are silicate minerals (Xie et al., 2011). Quartz was the main inorganic mineral, followed by carbonate and clay minerals, and a small amount of pyrite. In addition, the spectra from 5° and 29° also have the superposition of amorphous organic minerals. Generally speaking, compared to Huadian oil shale, the XRD diffraction peaks of inorganic minerals in Fuyu oil shale have sharp peaks, larger peaks, larger Full width at half maximum (FWHM) values and more inorganic minerals. Fuyu oil shale has better crystallization than Huadian oil shale, but its characteristic peaks have more overlaps. The peaks of the

diffraction peaks of quartz, calcite, pyrite and feldspar in Fuyu oil shale are obviously stronger than those in Huadian oil shale, indicating a more orderly arrangement of inorganic mineral grains in Fuyu oil shale, with more crystal planes in the same direction, and more obvious sedimentary features. The FWHM of inorganic minerals is affected by the grain size. The FWHM of quartz in Fuyu oil shale is larger than that in Huadian oil shale, which indicates that the quartz grain in Fuyu oil shale has large size. The grain size of other inorganic minerals is almost the same as that of inorganic minerals in Huadian oil shale. Moreover, the peak area of inorganic minerals in Fuyu oil shale is larger than that in Huadian oil shale, indicating more crystal planes and larger cell volume of different inorganic minerals and thus higher degree of crystallization in Fuyu oil shale.

2.2. Methods

The TG-DSC study of pyrolysis characteristics, kinetic parameters and product release properties of oil shale is of great significance to the optimum in-situ pyrolysis process for identifying process parameters to maximize oil yield. It is helpful to understand the effects of different heating rates, types and maturity of kerogen on pyrolysis characteristics, such as starting point, exothermic heat and pyrolysis stability of oil shale.

2.2.1. Pyrolysis characteristic parameters

According to the extrapolation method of TG-DTG, the initial pyrolysis temperature of oil shale can be determined by plotting the TG-DTG curve of oil shale through the following steps (Bai et al., 2015a). On the DTG curve of oil shale, the vertically intersected point B with the TG curve at the point where the weight loss rate is the highest. The tangent of the TG curve is made through point B. The tangent intersects with the extension line of the initial missed point A of the TG curve at point C. The temperature corresponding to point C is the ignition point of the oil shale. After the maximum weight loss rate of DTG curve, the weight loss rate decreases steadily at D point after the second stage of TG curve. The tangent line passing through point B intersects with point E, which is the final pyrolysis temperature of organic matter. As shown in Fig. 2 below, the pyrolysis interval diagrams of Fuyu and Huadian oil shales under nitrogen and air conditions are calibrated by extrapolation method.

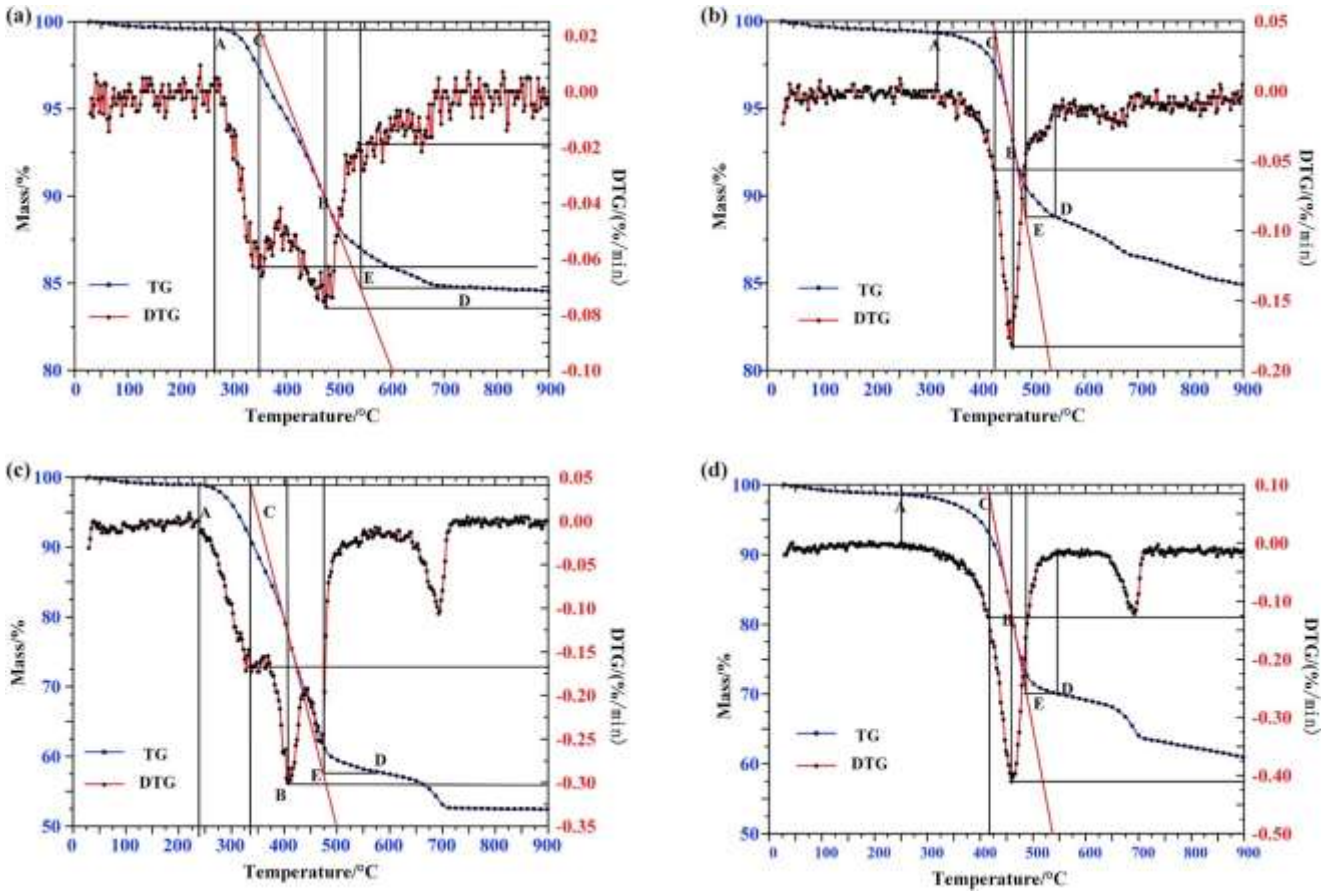

Fig. 2. Schematic diagram of extrapolation method to calibrate the pyrolysis interval of oil shale (10 °C/min).

2.2.2. Pyrolysis stability and exothermic analysis

Based on the measured data of pure carbon and the TG-DTG curve of oil shale samples, the evaluation index R_w and comprehensive pyrolysis index S are used to compare the pyrolysis stability of oil shale samples (Zhao et al., 2003).

$$R_w = \frac{655}{T_i} \times \frac{763}{T_{max}} \times \frac{(dm/dt)_{max}}{0.00582} \quad (1)$$

where, 655 is the ignition point of pure carbon, °C; 763 is the temperature corresponding to the maximum weight loss rate (0.00582) of pure carbon, °C; T_i is the initial pyrolysis temperature of oil shale, °C; $(dm/dt)_{Max}$ is the maximum weight loss rate of oil shale, %/min; and T_{max} is the corresponding temperature of the maximum weight loss rate of oil shale, °C.

$$S = \frac{(dm/dt)_{max}(dm/dt)_{mean}}{T_i^2 T_c} \quad (2)$$

$$\frac{dm}{dt} = \frac{m_2 - m_1}{t_2 - t_1} \quad (3)$$

$$\frac{dm}{dt} = \frac{(dm/dt)_i + (dm/dt)_c}{2} \quad (4)$$

T_c is the burnout temperature, °C; $(dm/dt)_i$ is the pyrolysis rate of ignition point, %/min; $(dm/dt)_C$ is the pyrolysis rate of burnout temperature, %/min. The relationship between endotherm and exotherm during oil shale pyrolysis can be obtained by analyzing DSC curve of oil shale pyrolysis , as shown in Fig. 3. (Xie et al., 2017).

$$\Delta H = \beta \int_0^{t_0} [\Delta T - (\Delta T)_c] = \beta S \quad (5)$$

where, ΔH is the accumulated exothermic process during the second stage of oil shale pyrolysis, J/g. β is 1, a dimensionless proportional constant, i.e. the effective heat transfer constant of proportionality between oil shale samples and measured metals. ΔT is the temperature difference between oil shale samples and reference metals, °C, i.e. the baseline of differential thermal curve. ΔTC is the temperature difference between the oil shale sample and the baseline of differential thermal analysis curve (DTC) curve, °C. S is the area of differential thermal peak of DSC curve, J/g.

2.2.3. Index and degree of pyrolysis

The pyrolysis index can be used to assess the pyrolysis performance of oil shale (Hong et al., 2016), which is defined as C_e.

$$C_e = \frac{f_1 \cdot f_2}{t_0} \quad (6)$$

$$f_2 = f - f_1 \quad (7)$$

Among them, f_1 is the ratio of organic matter content in oil shale to sample weight loss corresponding to ignition point on TG curve of oil shale. f_1 reflects the relative content of organic matter in oil shale. The higher the content of organic matter is, the better the pyrolysis performance is. t_0 is the time consumed during the pyrolysis of organic matter in oil shale on DTG curve. f is the total pyrolysis rate, i.e. the ratio of organic matter content to total weight loss in oil shale at t_0 moment of TG curve.

By analyzing the thermogravimetric curves of oil shale pyrolysis comprehensively, the pyrolysis degree C_i is constructed to characterize the pyrolysis process, which includes all the characteristic parameters for the whole of oil shale pyrolysis. The larger the value, the better the flammability and the fuller of the pyrolysis process (Khan, 1988).

$$c_i = \frac{(dm/dt)_{max}}{m_0 T_i T_c} \quad (8)$$

where, m_0 is the initial mass of the sample.

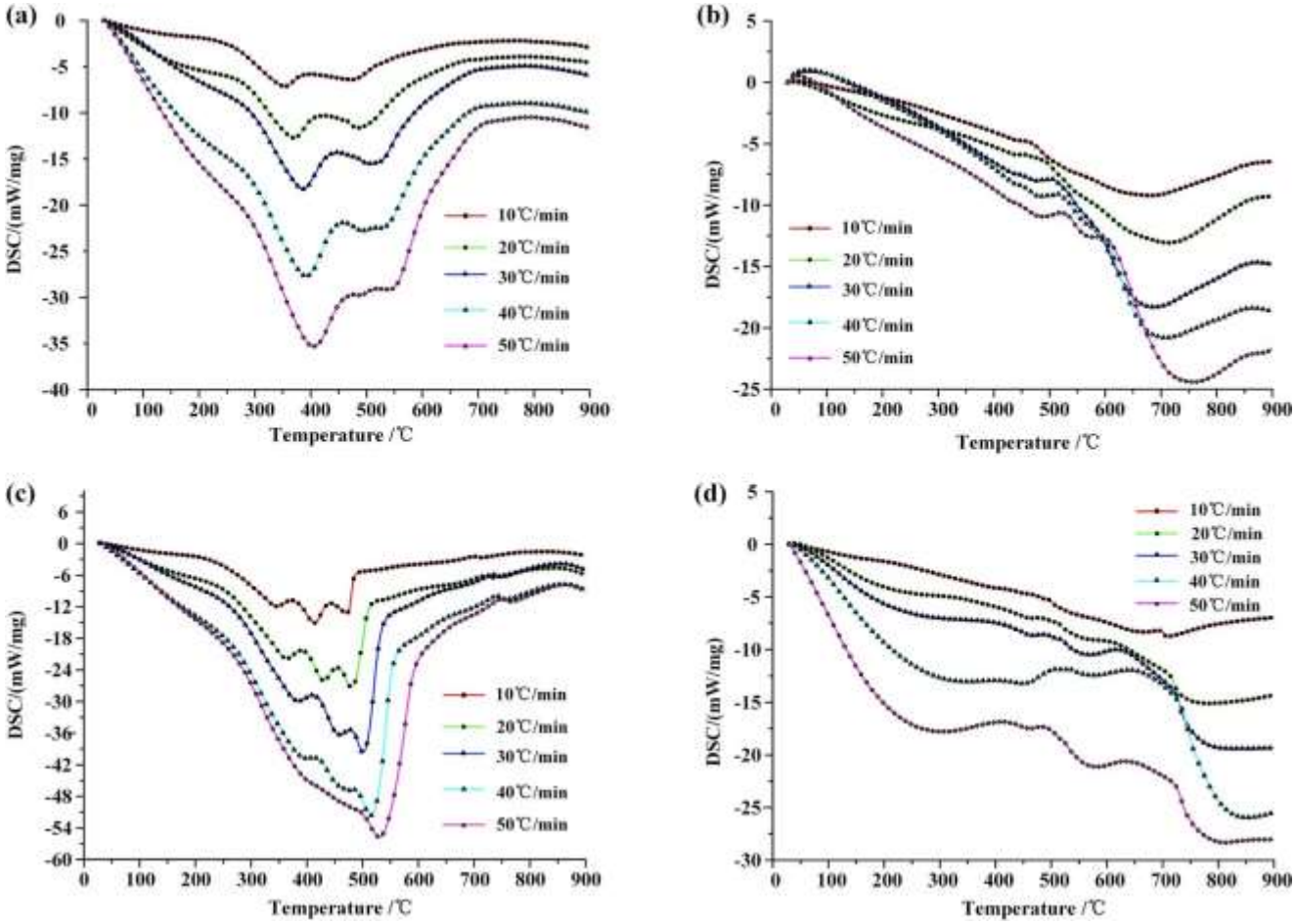

Fig. 3. DSC curves of Fuyu and Huadian oil shale under different atmospheres.

2.2.4. Release characteristics of products

In this paper, volatile release index I and reactivity index Ra are used to describe the difference of pyrolysis product release characteristics and conversion rate of oil shale in different areas under non-isothermal conditions (Ollero et al., 2002; Gomez-Barea et al., 2006; Gomez-Barea et al., 2006). In this paper, the release characteristics of oil shale pyrolysis products with conversion of 50% and 75% in the second stage are calculated.

$$I_{1/2} = \frac{R_a}{T_{max} T_i T_{1/2}} \tag{9}$$

$$\Delta T_{1/2} \rightarrow \frac{dm/dt}{R_a} = \frac{1}{2} \tag{10}$$

$$I_{3/4} = \frac{R_a}{T_{max} T_i T_{3/4}} \quad (11)$$

$$\Delta T_{3/4} \rightarrow \frac{dm/dt}{R_a} = \frac{3}{4} \quad (12)$$

$$R_a = -\frac{1}{m - m_\infty} \frac{dm}{dt} = \frac{1}{1-a} \frac{da}{dt} \quad (13)$$

$$a = \frac{m_o - m}{m_0 - m_\infty} \quad (14)$$

where, $\Delta T_{1/2}$ is the temperature range corresponding to 50% conversion, ^oC, also known as half peak width; $\Delta T_{3/4}$ is the temperature range corresponding to 75% conversion, ^oC. a is the conversion rate. m_0 represents the initial weight of the oil shale pyrolysis in second stage. m_∞ represents the final weight of the oil shale pyrolysis in second stage. m represents the weight at any time during the second stage of oil shale pyrolysis. Therefore, the above announcement reflects the characteristics of volatile matter released by instantaneous organic matter transformation during oil shale pyrolysis.

3. Results and discussion

3.1. Pyrolysis characteristic parameters

When the heating rates are 10 ^oC/min, 20 ^oC/min, 30 ^oC/min, 40 ^oC/ min and 50 ^oC/min, respectively, the TG-DTG curves of Fuyu and Huadian oil shales were measured in air and nitrogen atmosphere, as shown in Fig. 4 below. The pyrolysis parameters of Huadian and Fuyu oil shales obtained by extrapolation method are shown in Table 2 and Table 3 below.

Before the two oil shale samples reach the ignition point, it is the first weight loss stage, mainly the dehydration process. Because the water content of both oil shales is less than 4%, the dehydration is slow at this stage. After reaching the ignition point, the second stage of weight loss begins. The pyrolysis rate of kerogen increases obviously and the weight loss process is rapid. With the increase of heating rate, the pyrolysis zone of kerogen moves to the high temperature zone. In addition, compared to nitrogen, air helps to reduce the ignition point of oil shale and broaden the pyrolysis zone of organic matter. The third weight loss stage is the decomposition stage of clay minerals. Although the clay minerals are decomposed, other substances are not volatilized except bound water, so the weight loss stage is stable (Bai et al., 2015a, Bai et al., 2015; Liu et al., 2014. Jiang et al. (2006), Liu et al. (2014), and Yan et al. (2009) found similar results for Huadian oil shale. The phenomenon that the characteristic temperatures increase with the increase of heating rate is related to the heat transfer lag, and the higher the oil content, the more obvious the trend is.

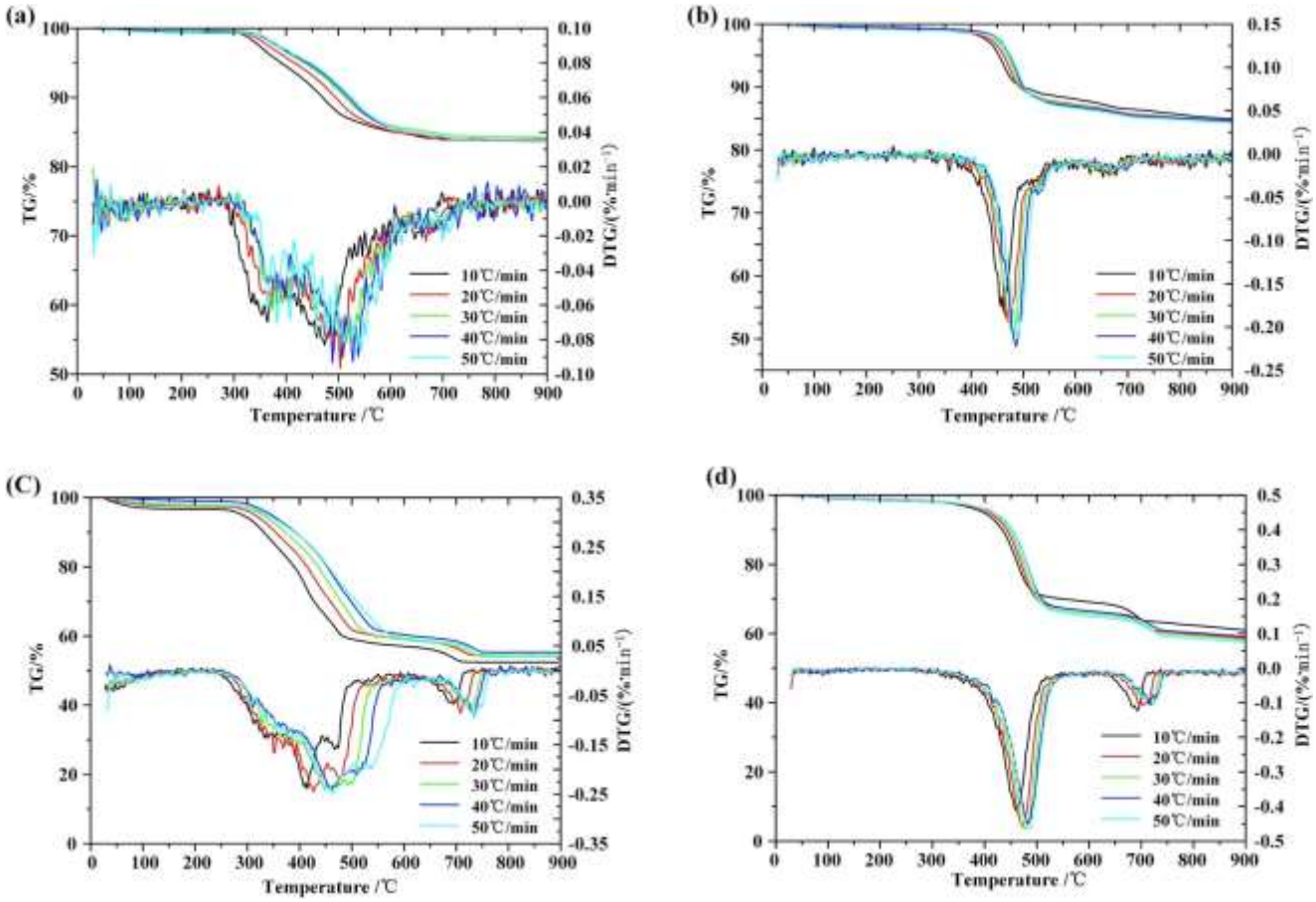

Fig. 4. TG-DTG curves of oil shale at different heating rates and atmospheres.

Table 2 Pyrolysis Characteristics of Oil Shale at Different heating Rates in Nitrogen Atmosphere.

Attribute	Heating rate °C/min	T_O/ °C	T_i/ °C	T_{max}/ °C	$(dm/dt)_{max}$ %/min	T_C/ °C
HD	10	283	419	460	0.415	524
	20	296	430	475	0.463	533
	30	304	437	479	0.471	541
	40	311	442	483	0.462	550
	50	325	448	486	0.477	561
FY	10	325	427	467	0.184	548
	20	343	439	476	0.195	560
	30	360	450	479	0.215	569
	40	375	454	485	0.224	567
	50	387	462	489	0.215	575

Table 3 Pyrolysis characteristics of oil shale under different heating rates in air atmosphere.

Attribute	Heating rate °C/min	T_O/ °C	T_i/ °C	T_{max}/ °C	$(dm/dt)_{max}$ %/min	T_C/ °C
HD	10	240	331	417	0.237	510
	20	245	342	427	0.256	524
	30	252	357	455	0.263	534
	40	257	365	465	0.271	552
	50	263	373	470	0.277	573
FY	10	270	350	474	0.077	531
	20	277	360	486	0.079	549
	30	289	375	502	0.083	563
	40	300	392	507	0.093	577
	50	309	400	525	0.087	591

3.2. Pyrolysis stability and exothermic analysis

In the second stage of pyrolysis, the calculation results of the evaluation indices RW and S for the pyrolysis stability of oil shale samples under different atmospheres and heating rates are shown in Fig. 5. Under these two atmospheric conditions, with the increase of heating rate, the evaluation indexes of oil shale pyrolysis stability decrease in varying degrees. Because the pyrolysis of oil shale moves to high temperature zone, and the corresponding ignition temperatures and the temperatures at the maximum pyrolysis rate increase.

Besides, oil content also affects the pyrolysis stability of oil shale. Under the same atmosphere, the pyrolysis stability of Huadian oil shale is higher than that of Fuyu oil shale because the oil content of Huadian oil shale is higher and the distribution of kerogen is more uniform. At the same heating rate, the temperature corresponding to ignition point and maximum pyrolysis rate is lower than that of Fuyu oil shale. With the same oil content, i.e. when the types of oil shale remain unchanged, the pyrolysis stability evaluation parameters of oil shale under nitrogen atmosphere are higher than those under air atmosphere. This is because the pyrolysis interval of oil shale is expanded and the maximum pyrolysis rate of oil shale is reduced under air atmosphere. However, under nitrogen atmosphere, the pyrolysis interval of oil shale is compact, and the maximum pyrolysis rate of oil shale is higher.

The peak area IDSC of the DSC curve can be obtained by integrating the curve, as shown in Fig. 6. The pyrolysis process of oil shale is exothermic, and the oil content has a certain influence on the exothermic process. Fuyu oil shale has a low oil content, and its exothermic process is lower than that of Huadian oil shale. Moreover, the exothermic process from oil shale pyrolysis under air atmosphere is higher than that under nitrogen atmosphere because oxygen in the air participates in the pyrolysis process of oil shale, and the oil and gas products by kerogen pyrolysis react

further to an oxidation that releases heat. However, under nitrogen atmosphere, the produced oil and gas products do not further oxidize, so the exothermic process is lower than that in air atmosphere.

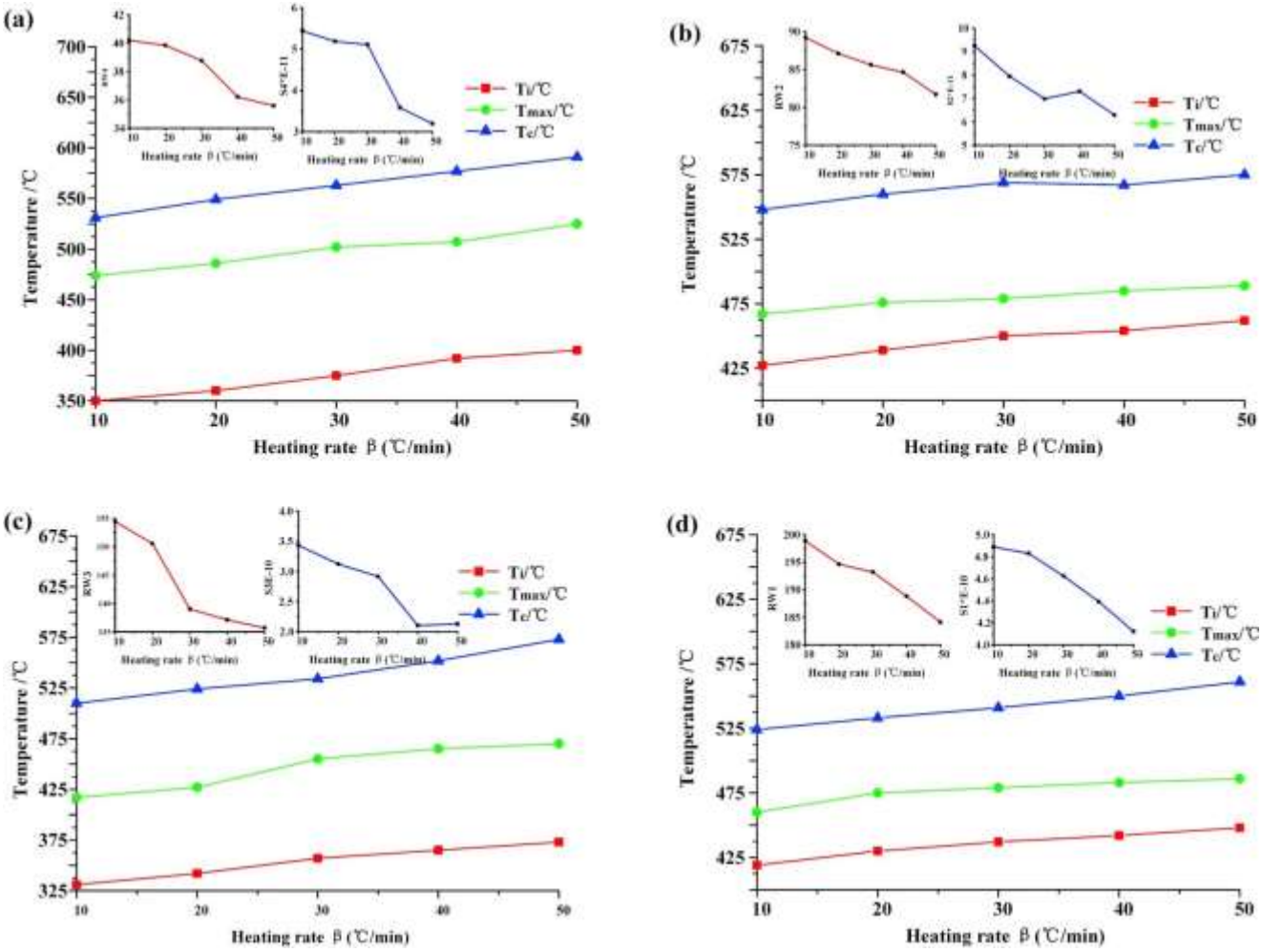

Fig. 5. Oil shale pyrolysis stability varies with heating rate and atmosphere.

The pyrolysis of oil shale is mainly concentrated in the second stage, but the pyrolysis interval of kerogen under nitrogen atmosphere is higher than that under air atmosphere. The pyrolysis reaction is more intense and the length of the interval is shortened. The exothermic activity is mainly concentrated in the pyrolysis stage of kerogen, i.e. the second stage of oil shale pyrolysis. With the increase of heating rate, the exothermic rate of oil shale also increases, as shown in Fig. 7, because when the heating rate is low, with the increase of temperature, part of the exothermic process from the thermal interpretation of kerogen is used for the orderly removal of chemical bonds, functional groups and side chains (branched chains) in molecular structure and the decomposition of clay minerals in oil shale.

The first is the chain breaking of weak chemical bonds and the precipitation of small molecules, especially gaseous products. With the increase of temperature, the precipitated organic

compounds are further decomposed, and these decomposition reactions are endothermic reactions. When the heating rate increases, the temperature gradient increases. The amount of pyrolysis of kerogen increases in unit time, and the side chains and the partially removed small molecular structures are displaced before further decomposition, so both the exothermic rate and the exothermic heat are increased. Similar results have been obtained by Kok (2007); Kok and Pamir (2003), where the effect of heating rate on the dynamics of oil shale was studied.

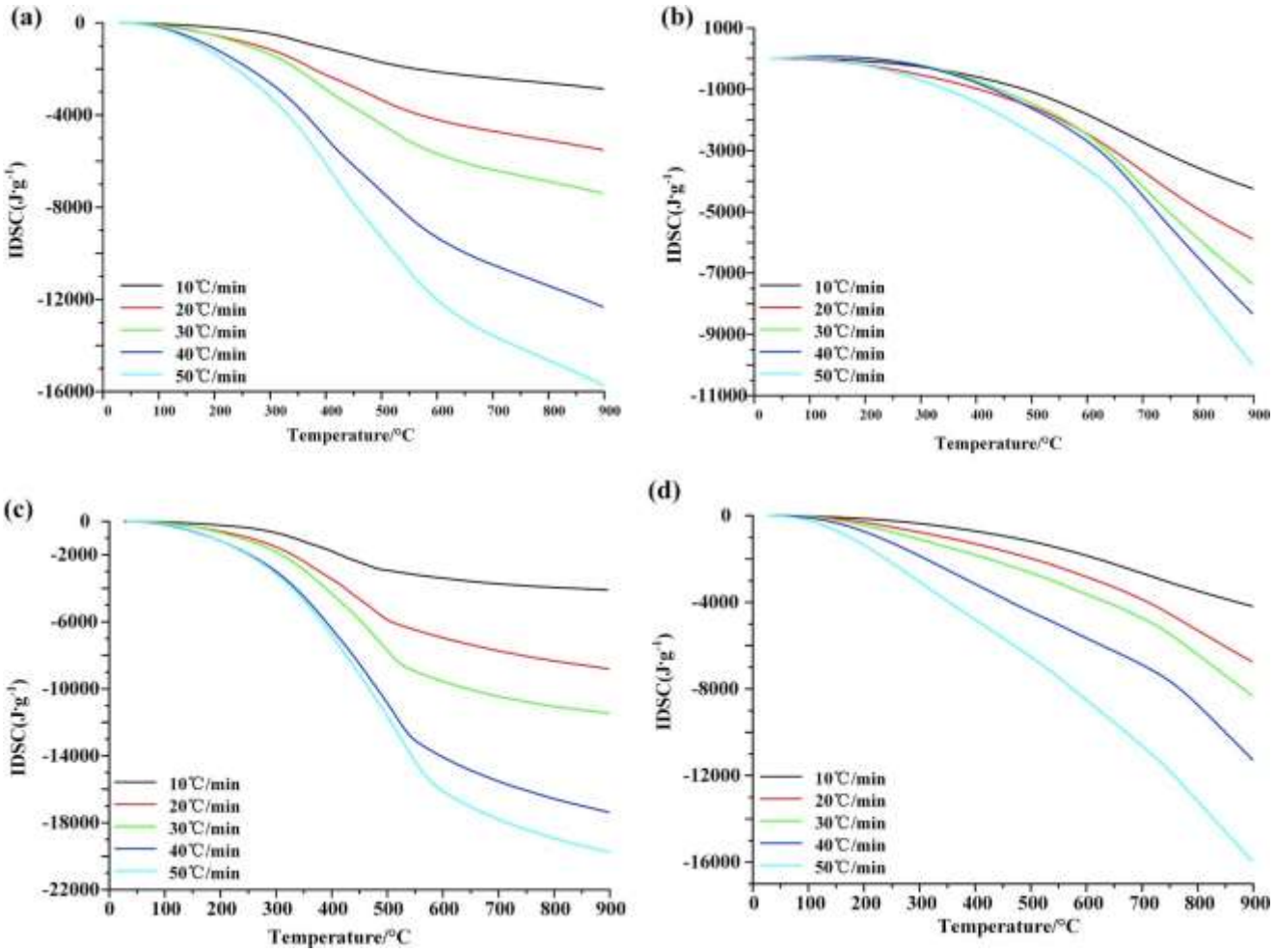

Fig. 6. Accumulated exothermic varies with heating rate and atmosphere.

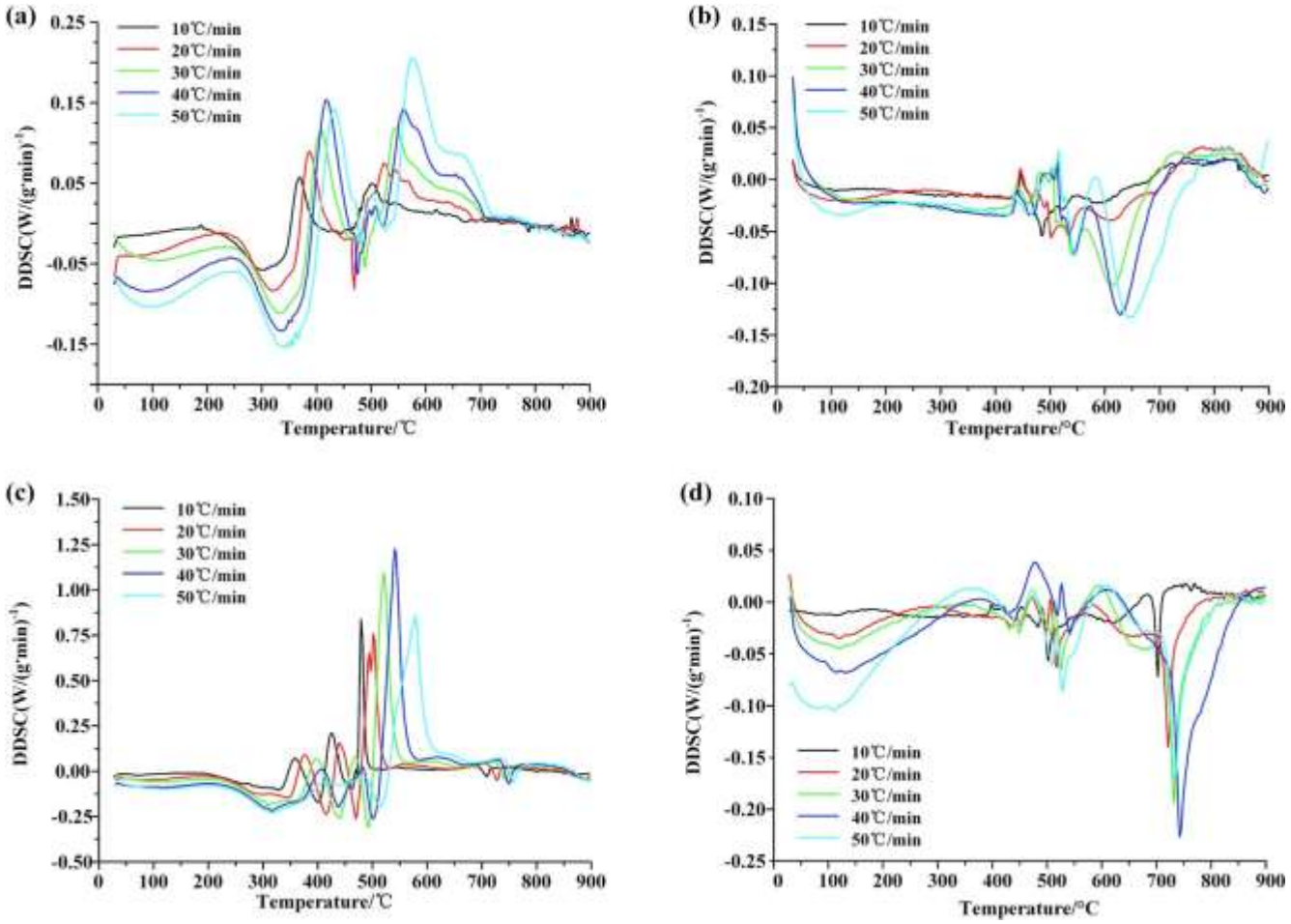

Fig. 7. Exothermic rate varies with heating rate and atmosphere.

3.3. Index and degree of pyrolysis

The higher the absolute value of pyrolysis index, the better performance of the pyrolysis. With the increase of heating rate, the ignition delay occurs, but the time consumed in the second stage of oil shale pyrolysis is greatly reduced. Therefore, with the increase of heating rate, the pyrolysis index of oil shale in the second stage increases.

As shown in Fig. 8, the pyrolysis index of Huadian oil shale with higher oil content is superior to that of Fuyu oil shale under both atmospheric conditions with different heating rates. This is because the oil content of Huadian oil shale is as high as 18.7%, and the distribution of kerogen is more average. The pyrolysis process is relatively stable and affected by the pyrolysis time. The oil content of Fuyu oil shale is only 4.7%, and the distribution of kerogen is not uniform, so the pyrolysis trend is not significant. In addition, the pyrolysis index is also affected by pyrolysis atmosphere. Generally speaking, the pyrolysis index under air atmosphere is higher than that under nitrogen atmosphere due to the combustion-supporting effect from oxygen in air. At the same heating rate, the consumption of kerogen per unit time in the second stage of oil shale pyrolysis increases, and the pyrolysis time decreases, so the pyrolysis index increases.

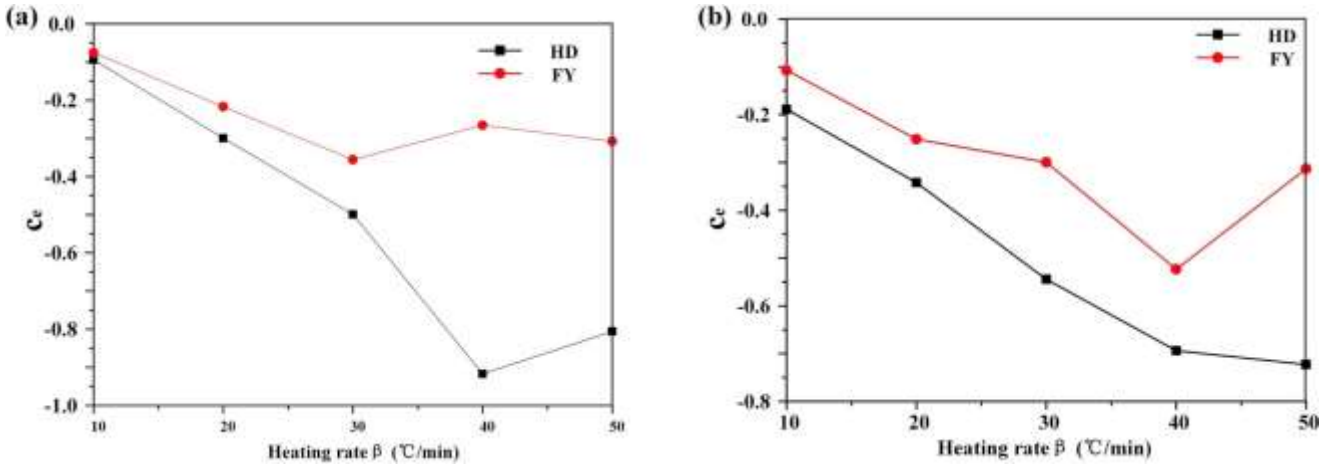

Fig. 8. Pyrolysis indices of oil shales at different heating rates and atmospheric conditions.

Oil shale is a complex mixture of various minerals and organic matter. The content and type of organic matter affect the difficulty and speed of pyrolysis. The heating rate has similar effect on the maximum pyrolysis rate and degree of oil shale. As shown in Fig. 9, The maximum pyrolysis rate and degree of Fuyu oil shale reach the maximum when the heating rate is 40 °C/min. When the heating rate is 20 °C/min, the pyrolysis degree of Huadian oil shale reaches its maximum value, and the maximum pyrolysis rate still increases with the increase of heating rate. The maximum pyrolysis rate reaches the maximum when the heating rate reaches 50 °C/min. The main reason for this phenomenon is due to the difference of oil contents of these two types of oil shales. Fuyu oil shale has low oil content and uneven distribution of kerogen. When the pyrolysis rate increases, the pyrolysis time of the second stage decreases, so the pyrolysis of kerogen is more concentrated, showing a better pyrolysis trend. Huadian oil shale has a high oil content. In theory, the increase of heating rate leads to the decrease of pyrolysis time. Huadian oil shale has a better pyrolysis degree. However, due to the high oil content of Huadian oil shale and the uniform distribution of kerogen, the whole pyrolysis process of Huadian oil shale is uniform and slow. With the increase of heating rate, pyrolysis time decreases, leading to concentrated pyrolysis of Huadian oil shale and non-uniform heat flux profiles, and thus resulting in incomplete pyrolysis of the oil shale. Therefore, the pyrolysis degree tends to decrease with the increase of heating rate. Under nitrogen atmosphere, Huadian oil shale has the best pyrolysis degree only when the heating rate is between 20 and 30 °C/ min. Under air atmosphere, the optimum pyrolysis state can be achieved at the heating rate of 20 °C/min, which is due to the combustion-supporting effect of oxygen. Nitrogen has no combustion-supporting effect, so the heating rate is slightly higher than 20 °C/min before reaching the optimal pyrolysis state.

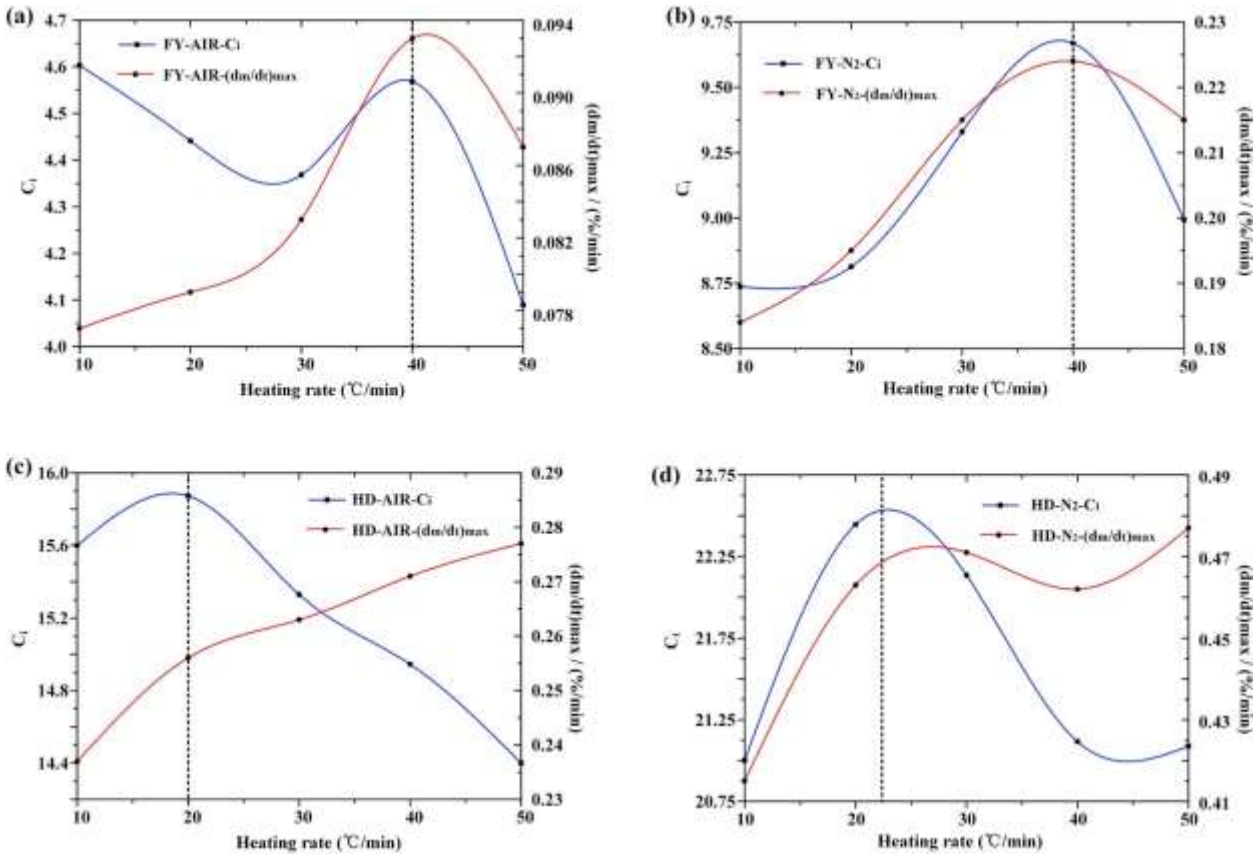

Fig. 9. Degree of oil shale pyrolysis varies with heating rate and atmosphere.

3.4. Release characteristics of products

In the second stage of oil shale pyrolysis, the release characteristic index I0.5 and I0.75 increase almost linearly with the increase of heating rate. As shown in Fig. 10, this is because the increase of heating rate shortens the time of the second stage of oil shale pyrolysis, and the pyrolysis reaction is intensified and the product release is concentrated.

The release indices of the products are different under two atmospheric conditions. Under the condition of nitrogen, the product release characteristic index of the same conversion rate is higher than that under the air. This is because when air is used, oxygen has combustion-supporting effect, prolonging the pyrolysis interval of the second stage of oil shale. The oil shale in the same area has the same oil content. As the pyrolysis interval becomes longer, so is the product release interval, hence the maximum product release rate is reduced. Under nitrogen atmosphere, the interval of the second stage of oil shale pyrolysis is more intense than that under air atmosphere. This is conducive to the concentrated release of products, so the maximum release rate of products becomes higher. In addition, when the pyrolysis interval of the second stage of oil shale is prolonged, the half peak width $\Delta T_{1/2}$ and $\Delta T_{3/4}$ at 50% and 75% conversion rates is also increased. Combining these two characteristics, the index of product release characteristics under air condition decreases.

Moreover, under the same atmosphere, with the increase of pyrolysis conversion in the second stage of oil shale, the release characteristic index of products decreases. This is because with the increase of heating rate, the pyrolysis reaction of oil shale in the second stage moves to the high temperature zone, which leads to the increase of half peak width $\Delta T_{1/2}$ and $\Delta T_{3/4}$ corresponding to conversion of 50% and 75%. Although the maximum product release rate also increases, the degree of the increased product release rate is less than the degree to which the pyrolysis reaction moves to the high temperature zone. Therefore, with the increase of conversion, the release characteristic index of the product decreases. Liao and Ma (2010), Chen et al. (2011), Wang et al. (2013) reported the same finding in pyrolysis experiments of organic matter.

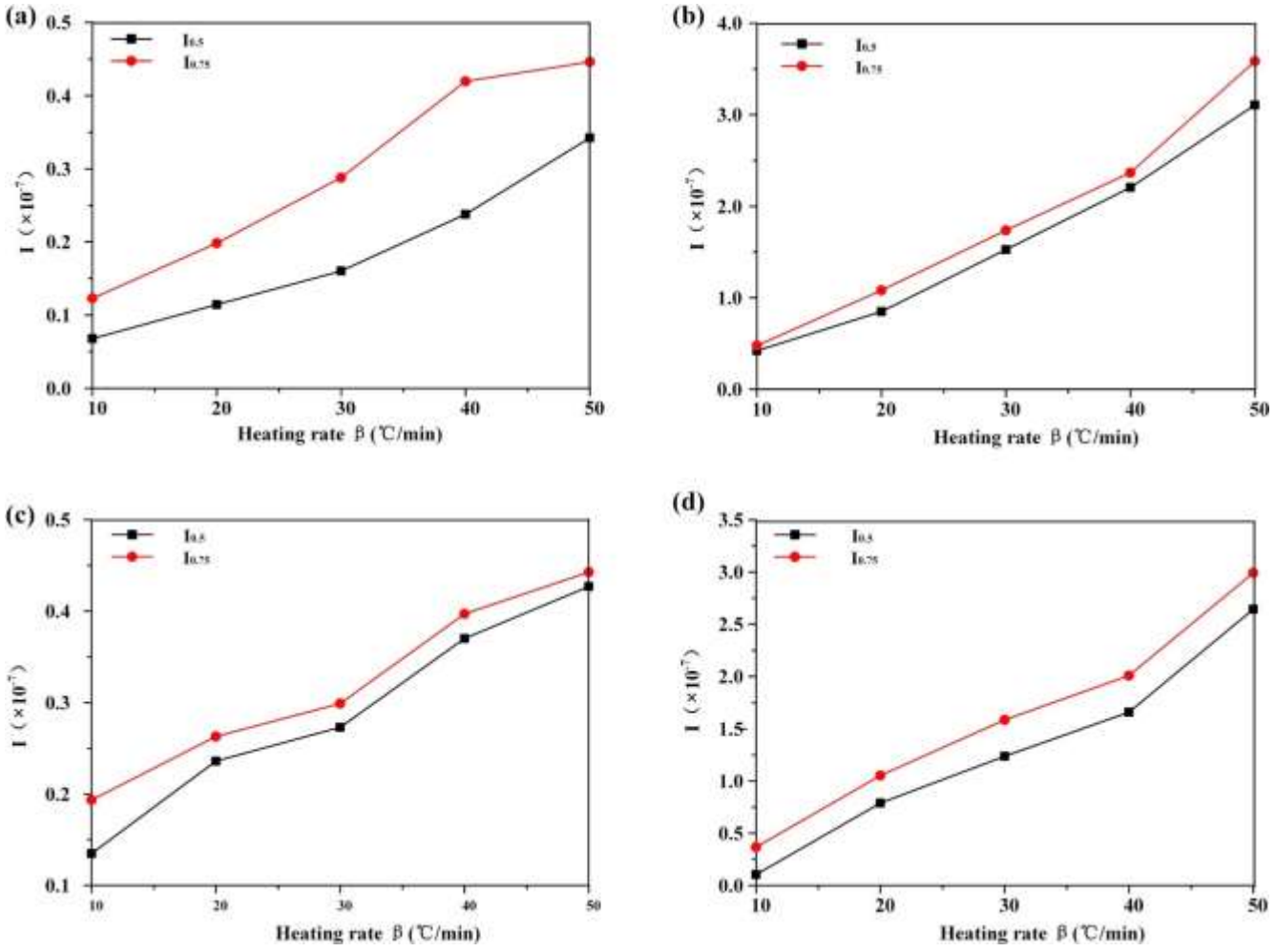

Fig. 10. Volatile release characteristics in the second stage of oil shale pyrolysis.

4. Conclusion

Under non-isothermal conditions, increasing heating rate causes oil shale pyrolysis moving to higher temperature zone. This trend is more noticeable at the higher oil content. Higher oil content leads to more stable pyrolysis of oil shale. The pyrolysis under nitrogen atmosphere is more stable than that under air atmosphere. Air prolongs the pyrolysis interval of oil shale, which

leads to the decrease of maximum pyrolysis rate. Under nitrogen atmosphere, the pyrolysis interval of oil shale is more intense. The pyrolysis process of oil shale is exothermic, and the higher the oil content, the higher the exothermic rate. The starting temperature of the second stage pyrolysis of oil shale is lower under air atmosphere, and the combustion-supporting effect of oxygen makes the pyrolysis process to take on a more stable mode. Huadian oil shale has a higher oil content and a higher pyrolysis index than those of Fuyu oil shale. The pyrolysis index of oil shale increases with the increase of heating rate, and the degree of pyrolysis first increases and then decreases. The optimum heating rate that produces the highest oil product yield for pyrolysis progress of Huadian oil shale is 20 ^{o}C/min, and Fuyu oil shale is 40 ^{o}C/min. Under nitrogen atmosphere, the release characteristic index of products with the same conversion rate is higher than that under air atmosphere. In addition, with the increase of heating rate, the pyrolysis time of oil shale decreases and the products are released centrally, thus leading to increases of the release characteristic index of products.

Acknowledgments

The authors would like to gratefully acknowledge the support provided by the Fuyu oil shale base of Jilin University in the course of this experiment, Jilin Provincial Science and Technology Department Project (20130302030SF), Science and technology innovation team of Jilin University (2017TD-13), and Interdisciplinary Research Grant Scheme for Doctoral Students of Jilin University (10183201839). The authors also express their appreciation to technical reviewers for their constructive comments. Finally, we would like to thank Chen Dejiang for his help during the experiment.

Appendix A. Supplementary data

Supplementary data to this article can be found online at https://doi.org/10.1016/j.petrol.2019.106812.

References

Altun, N Emre, Hwang, Jiann-Yang, Cahit, Hicyilmaz, 2009. Enhancement of flotation performance of oil shale cleaning by ultrasonic treatment. Int. J. Miner. Process. 91 (1–2), 1–13. https://doi.org/10.1016/j.minpro.2008.10.003.

Bai, F.T., Sun, Y.H., Liu, Y.M., et al., 2013. Basic Physicochemical Characteristics of the Huadian Oil Shales, z1. Exploration Engineering (Rock & Soil Drilling and Tunneling), pp. 239–243.

Bai, Fengtian, Guo, Wei, Xiaoshu, Lü, et al., 2015b. Kinetic study on the pyrolysis behavior of Huadian oil shale via non-isothermal thermogravimetric data. Fuel 146, 111–118. https://doi.org/10.1016/j.fuel.2014.12.073.

Bai, Jingru, Shao, Jiaye, Zhang, Hongxi, et al., 2017. TG-FTIR research OF alkaline lignin and oil shale CO-pyrolysis synergy action. Acta Energiae Solaris Sin. 38 (6), 1533–1538.

Bao, Jia, Jyun-Syung, Tsau, Reza, Barati, 2019. A review of the current progress of CO2 injection EOR and carbon storage in shale oil reservoirs. Fuel 236, 404–427. https://doi.org/10.1016/j.fuel.2018.08.103.

Bai, Fengtian, Sun, Youhong, Liu, Yumin, et al., 2015a. Thermal and kinetic characteristics of pyrolysis and combustion of three oil shales. Energy Convers. Manag. 97, 374–381. https://doi.org/10.1016/j.enconman.2015.03.007.

Chen, C.X., Ma, X.Q., Liu, K., 2011. Thermogravimetric analysis of microalgae combustion under different oxygen supply concentrations. Appl. Energy 88, 3189–3196. https://doi.org/10.1016/j.apenergy.2011.03.003.

Dong, Liang Zhong, Wen, Chun Wang, Zhen, Lin Zou, et al., 2018. Investigation on methane recovery from low-concentration coal mine gas by tetra-n-butyl ammonium chloride semiclathrate hydrate formation. Appl. Energy 227, 686–693. https://doi.org/10.1016/j.apenergy.2017.08.069.

Gomez-Barea, A., Ollero, P., Fernandez-Baco, C., 2006a. Diffusional effects in CO_2 gasification experiments with single biomass char particles. 1.Experimental investigation. Energy Fuels 20, 2202–2210. https://doi.org/10.1021/ef050365a.

Gomez-Barea, A., Ollero, P., Villanueva, A., 2006b. Diffusional effects in CO2 gasification experiments with single biomass char particles. 2. Theoretical predictions. Energy Fuels 20, 2211–2222. https://doi.org/10.1021/ef0503663.

Hong, Chen, Wang, Zhi-qiang, Xing, Yi, et al., 2016. Effects of different additives on co-combustion of pulverized coal-sludge and kinetic analysis. J. China Coal Soc. 41 (11), 2853–2859.

Jiang, X.M., Han, X.X., Cui, Z.G., 2006. Mechanism and mathematical model of Huadian oil shale pyrolysis. J. Therm. Anal. Calorim. 86, 457–462. https://doi.org/10.1007/ s10973-005-7065-1.

Juliana, Pedrilho Foltin, Antonio, Carlos Luz Lisboa, de Klerk, Arno, 2017. Oil shale pyrolysis: conversion dependence of kinetic parameters. Energy Fuels 31 (7), 6766–6776. https://doi.org/10.1021/acs.energyfuels.7b00578.

Khan, Mr, 1988. Correlation between refractive-indexes and other fuel-related physical and chemical-properties OF pyrolysis liquids derived from coal, oil-shale, and tar sand. Abstr. Pap. Am. Chem. Soc. 195, 83–84.

Kok, M.V., 2007. Heating rate effect on the DSC kinetics of oil shales. J. Therm. Anal. Calorim. 90, 817–821. https://doi.org/10.1007/s10973-007-8240-3.

Kok, M.V., Pamir, R., 2003. Pyrolysis kinetics of oil shales determined by DSC and TG/ DTG. Oil Shale 20, 57–68.

Liao, Y.F., Ma, X.Q., 2010. Thermogravimetric analysis of the co-combustion of coal and paper mill sludge. Appl. Energy 87, 3526–3532. https://doi.org/10.1016/j. apenergy.2010.05.008.

Liu, Q.Q., Han, X.X., Li, Q.Y., Huang, Y.R., Jiang, X.M., 2014. TG-DSC analysis of pyrolysis process of two Chinese oil shales. J. Therm. Anal. Calorim. 116, 511–517. https://doi.org/10.1007/s10973-013-3524-2.

Ollero, P., Serrera, A., Arjona, R., et al., 2002. Diffusional effects in TGA gasification experiments for kinetic determination. Fuel 81, 1989–2000. https://doi.org/10.1016/S0016-2361(02)00126-6.

Omar, S.Al-Aye, Suliman, Mohd R., AbdelRahman, Nafi, 2010. Kinetic modeling of liquid generation from oil shale in fixed bed retort. Appl. Energy 87 (7), 2273–2277. https://doi.org/10.1016/j.apenergy.2010.02.006.

Sun, Youhong, Bai, Fengtian, Liu, Baochang, et al., 2014. Characterization of the oil shale products derived via topochemical reaction method. Fuel 115, 338–346. https://doi.org/10.1016/j.fuel.2013.07.029.

Sun, Youhong, Bai, Fengtian, Xiaoshu, Lü, et al., 2015. Kinetic study of Huadian oil shale combustion using a multi-stage parallel reaction model. Energy 82 (c), 705–713. https://doi.org/10.1016/j.energy.2015.01.080.

Wang, Qing, Jia, Chunxia, Liu, Hongpeng, 2012. Combustion kinetic model of wangqing oil shale. Proceed. CSEE 32 (23), 27–31. 10.4028/www.scientific.net/AMM .529.272, 146.

Wang, C.A., Du, Y.B., Che, D.F., 2013. Reactivities of coals and synthetic model coal under oxy-fuel conditions. Thermochim. Acta 553, 8–15. https://doi.org/10.1016/j. tca.2012.11.023.

Xie, Fangfang, Wang, Ze, Song, Wenli, et al., 2011. FTIR analysis of oil shales from Huadian Jilin and their pyrolysates. Spectrosc. Spectr. Anal. 1, 91–94. https://doi.org/10.3964/j.issn.1000-0593(2011)01-0091-04.

Xie, Qiang, Ding-cheng, Liang, Lu, He, et al., 2017. Measurement of coal pyrolysis reaction heat by TG-DSC. J. China Coal Soc. 42 (2), 538–546.

Xiong, yao, Ma, Mingjie, Zhao, Di, et al., 2015. Pyrolysis features of oil shale from Yaojie and the pyrolysate analysis. Acta Pet. Sin. 1, 98–103.

Yan, J.W., Jiang, X.M., Han, X.X., 2009. Study on the characteristics of the oil shale and shale char mixture pyrolysis. Energy Fuels 23, 5792–5797. https://doi.org/10.1021/ ef9008345.

Zhang, Xiangping, Li, Chunshan, Zhang, Suojiang, et al., 2018. Practices for modeling oil shale pyrolysis and kinetics. Rev. Chem. Eng. 34 (1), 21–42. https://doi.org/ 10.1515/revce-2016-0038. DOI 10.1515/revce-2016-0038.

Zhao, Hong, Yang Jian, guo, Chang, Ai ying, et al., 2003. Establishment of combustion stability index of pulverized coal. J. Combust. Sci. Technol. 9 (4), 364–366,